Sleep architecture changes in the APP23 mouse model manifest at onset of cognitive deficits

Van Erum, Jan; Van Dam, D.; Sheorajpanday, R.; De Deyn, Peter Paul

Published in:
Behavioural Brain Research

DOI:
10.1016/j.bbr.2019.112089

Publication date:
2019

Behavioural Brain Research 373 (2019) 112089

Contents lists available at ScienceDirect

Behavioural Brain Research

journal homepage: www.elsevier.com/locate/bbr

Sleep architecture changes in the APP23 mouse model manifest at onset of cognitive deficits

Jan Van Erum[a], Debby Van Dam[a,b], Rishi Sheorajpanday[a], Peter Paul De Deyn[a,b,c,*]

[a] Laboratory of Neurochemistry and Behavior, Institute Born-Bunge, Department of Biomedical Sciences, University of Antwerp, Wilrijk (Antwerp), Belgium
[b] Department of Neurology and Alzheimer Center, University of Groningen and University Medical Center Groningen (UMCG), Groningen, the Netherlands
[c] Department of Neurology, Memory Clinic of Hospital Network Antwerp (ZNA) Middelheim and Hoge Beuken, Antwerp, Belgium

ARTICLE INFO

Keywords:
Sleep
Cognition
Locomotor activity
APP23
Morris water maze
EEG

ABSTRACT

Alzheimer's disease (AD), which accounts for most of the dementia cases, is, aside from cognitive deterioration, often characterized by the presence of non-cognitive symptoms such as activity and sleep disturbances. AD patients typically experience increased sleep fragmentation, excessive daytime sleepiness and night-time insomnia. Here, we sought to investigate the link between sleep architecture, cognition and amyloid pathology in the APP23 amyloidosis mouse model for AD. By means of polysomnographic recordings the sleep-wake cycle of freely-moving APP23 and wild-type (WT) littermates of 3, 6 and 12 months of age was examined. In addition, ambulatory cage activity was assessed by interruption of infrared beams surrounding the home cage. To assess visuo-spatial learning and memory a hidden-platform Morris-type Water Maze (MWM) experiment was performed. We found that sleep architecture is only slightly altered at early stages of pathology, but significantly deteriorates from 12 months of age, when amyloid plaques become diffusely present. APP23 mice of 12 months old had quantitative reductions of NREM and REM sleep and were more awake during the dark phase compared to WT littermates. These findings were confirmed by increased ambulatory cage activity during that phase of the light-dark cycle. No quantitative differences in sleep parameters were observed during the light phase. However, during this light phase, the sleep pattern of APP23 mice was more fragmented from 6 months of age, the point at which also cognitive abilities started to be affected in the MWM. Sleep time also positively correlated with MWM performance. We also found that spectral components in the EEG started to alter at the age of 6 months. To conclude, our results indicate that sleep architectural changes arise around the time the first amyloid plaques start to form and cognitive deterioration becomes apparent. These changes start subtle, but gradually worsen with age, adequately mimicking the clinical condition.

1. Introduction

World's leading cause of dementia, Alzheimer's disease (AD), is a progressive, neurodegenerative disorder affecting an increasing aged population. Apart from the characteristic cognitive decline, up to 60% of AD patients experience sleep and circadian rhythm disturbances [1,2]. Compared to healthy aging, AD is associated with increased sleep fragmentation, excessive daytime sleepiness and night-time insomnia [3–7]. Non-rapid eye movement (NREM) and rapid eye movement (REM) sleep are quantitatively reduced, resulting in a reduced total sleep time (TST) [6]. Moreover, the deepest stages of NREM sleep, also referred to as slow wave sleep (SWS), are often absent [6], resulting in a diminished sleep efficiency. Additionally, circadian dysrhythmia might lead to the emergence of the 'sundowning' phenomenon, which can ultimately lead to a complete reversal of the day-night cycle in these patients. Sleep disorders and sundowning decrease the self-care ability of AD patients, are among the main reasons for caregiver exhaustion, and greatly impact the rate of institutionalization [8,9].

Sleep and circadian rhythm disturbances already occur in early stages of probable AD and parallel the progressive cognitive decline [8,10]. Sleep abnormalities are often considered to be a consequence of AD pathology [11–13]. However, sleep is important to remove toxic proteins and peptides from the brain [14]. Accordingly, studies have demonstrated that sleep loss can increase interstitial fluid amyloid-beta (Aβ) and, consequently, plaque burden [15]. Therefore, it is suggested that amyloid plaque formation alters Aβ dynamics, resulting in a disturbed sleep-wake cycle, thereby exacerbating the accumulation of toxic proteins and the progression of the pathology [16]. Moreover, sleep processes are presumed to participate in memory consolidation, an active process that relies on reactivation and reorganization of newly

* Corresponding author at: Campus Drie Eiken, Universiteitsplein 1, 2610 Wilrijk, Belgium.
E-mail address: p.p.de.deyn@umcg.nl (P.P. De Deyn).

https://doi.org/10.1016/j.bbr.2019.112089
Received 7 May 2019; Received in revised form 26 June 2019; Accepted 16 July 2019
Available online 17 July 2019

encoded representations [17]. Disruption of sleep interferes with cognitive abilities, even in healthy young people [18]. Thus, extensively reduced amounts of sleep will aggravate cognitive decline in AD even more.

The APP23 amyloidosis mouse model has already been thoroughly characterized and mimics many clinical AD symptoms [19]. Hemizygous (HEM) APP23 display scarce Aβ deposits from 6 months of age. They increase in size and number with aging, until an extensive area of the neocortex and hippocampus is occupied by amyloid deposits at 24 months of age. Moreover, amyloid deposits in cerebral vasculature, also known as cerebral amyloid angiopathy, start to form from 9 months of age and increase with age [19–21]. Here, we aimed to further understand the contribution of amyloid pathology to sleep regulation and circadian function, and its influence on acquisition and retrieval of memory in AD. We, therefore, established whether APP23 mice display age-related disruptions in baseline sleep architecture and circadian distribution of sleep and activity. Furthermore, we examined whether these changes correlate with spatial learning and memory capacities and spectral components in the electroencephalogram (EEG).

2. Materials and methods

2.1. Animal model

The transgenic APP23 amyloidosis mouse model of AD carries the human APP gene containing the Swedish mutation (KM670/671 N L) on a C57BL/6 J background. The expression is under control of the murine neuronal Thy1 promotor [21], which results in approximately tenfold overexpression of APP in the hippocampus of HEM vs wild-type (WT) controls. In addition, the cortical APP expression steadily increments with age, with a 2-fold overexpression at 6–8 weeks and 20-fold overexpression at 24 months [22]. Male, HEM APP23 mice and their WT littermates of 3 (WT: $n = 10$, HEM: $n = 11$), 6 (WT: $n = 12$, HEM: $n = 10$) and 12 (WT: $n = 11$, HEM: $n = 11$) months of age were bred and aged in our facilities. The amyloid load of these mice increases with age, with no amyloid deposition at 3 months and extensive amyloid plaques at 12 months of age. All mice were group-housed in standard mouse cages under conventional laboratory conditions, and individually housed from the day of electrode implantation; constant room temperature (22 ± 2 °C), humidity level (55 ± 5%), 12 h/12 h day/night cycle (lights on at 8 a.m.). Food and water were supplied ad libitum. Custom primers (Biolegio, The Netherlands) were used for genotyping by PCR analysis performed, on DNA extracted from ear punches, collected from mice aged 4 weeks. All experiments were carried out in compliance with the European Community Council Directive (2010/63/EU) and were approved by the Animal Ethics Committee of the University of Antwerp (ECD approval n° 2011/49).

2.2. Video EEG recording

By stereotactic surgery, two active screw EEG electrodes (E363/96/1.6, Plastics One Inc., Roanoke, USA) were implanted over the frontal and parietal cortices, while one ground and one reference electrode were placed over the cerebellum (*coordinates from reference point Bregma: right frontal cortex: anteroposterior (AP) +2.0 mm, mediolateral (ML) +2.0 mm; right parietal cortex: AP – 2.0 mm, ML +2.0 mm; ground electrode: AP – 4.90 mm, ML 0.0 mm; reference electrode: AP – 6.70 mm, ML 0.0 mm*) [23]. Two EMG electrodes (E363/76/SPC, Plastics One Inc., Roanoke, USA) were inserted into the nuchal muscles. All implanted electrodes were fixed to the skull with carboxylate cement (Durelon™, 3 M ESPE S.A., Germany). The sockets were attached to an electrode pedestal (MS 363, Plastics One, Roanoke, V.S.) and the assembly was secured to the skull by carboxylate cement (Durelon™, 3 M ESPE S.A., Germany). Postoperatively, animals were housed individually and carefully monitored for pain and distress.

After a seven-day recovery period, video EEG of freely-moving APP23 and WT mice commenced with three days of habituation in the EEG recording room. Then, baseline EEG was recorded with a 40-channel EEG headbox (Large EEG headbox, Schwarzer Ahns, Germany) for 72 h, of which only the last 24 h were included into the sleep analysis. Additionally, the experiment was recorded with a video camera (DCR-DVD105 DVD Handycam camcorder with 20x optical zoom and infrared lens, Sony). Via a video converter (Canopus ADVC55), the analog signal was digitally converted. In the BrainRT™ software the video was synchronized with the recorded EEG. The video was used to check for abnormalities during the recordings and to assist during vigilance scoring. The EEG signal was sampled at a rate of 250 Hz and band-pass filtered between 0.5 and 30 Hz. Scoring of sleep stages was performed manually and off-line in 4-s epochs by visual inspection of the raw EEG an EMG signal in BrainRT™ (OSG BVBA, Rumst, Belgium). In our experience, automated sleep scoring is around 20% less accurate than manual scoring and therefore the latter was preferred. The vigilance states were defined as follows: (1) wake (EEG with low amplitude (A), high frequency (f) EEG; high EMG activity), (2) NREM (EEG with high A, low f; low EMG activity), (3) REM (EEG with low A, high f; low EMG activity) [24]. The minimal interruption criteria were applied to determine the vigilance state episodes as previously described [25,26]. The individual sleep parameters were calculated for both the light and dark phase. Sleep fragmentation was defined as the number of brief awakenings (i.e. waking episodes shorter than 16 s).

The 24 -h scored EEG signals were downsampled to 125 Hz and subjected to Fast Fourier transform (FFT) in BrainRT™ to generate delta (0.5–3.5 Hz), theta (3.5–7.5 Hz), alpha (7.5–12.5 Hz) and beta (12.5–30 Hz) band power in wake, NREM and REM. These frequency ranges are routinely applied in a (pre)clinical setting [27–29]. A four-second epoch window (that corresponded with the sleep scoring window) with Hanning filter and FFT size of 512 was used. Power was calculated from 0 to 62.5 Hz with a 0.244 Hz bin width. Power was expressed relatively to the sum of all band power values (%), to minimize variations in oscillatory amplitude between animals.

2.3. Ambulatory cage activity

Horizontal locomotor activity was tracked in the EEG recording chamber using three infrared sensors. The number of beam crossings was counted in 4 s bins.

2.4. Morris water maze

Three days after polysomnography, evaluation of spatial learning and memory was initiated by means of the hidden platform Morris Water Maze (MWM) test [30]. In this experimental setup, a circular pool (diameter: 150 cm, height: 30 cm) was filled with opacified water, kept at 25 °C, in which a Perspex platform (diameter 15 cm) was placed in one of the quadrants. The water surface is 1 cm above the platform and the MWM is surrounded by invariable visual cues. Acquisition training consisted of eight trial blocks (during two weeks) of four daily trials starting from four different positions in a quasi-random order with a 15-min intertrial interval. During the first week of the MWM, all mice underwent 4 consecutive trial blocks, one trial block each day. After a 3-day interval, again 4 consecutive trial blocks were performed during week two. During these training trials the escape latency to the platform, path length and swim speed was measured using a computerized video-tracking system ((Ethovision 6, Noldus, Wageningen, the Netherlands). If a mouse was not able to reach the platform within 120 s, it was placed on the platform, where it stayed for 15 s before being returned to its home cage. Four days after the last trial block, the acquisition phase was followed by a probe trial, in which the platform was removed from the maze, and in which the animals were allowed to swim freely for 100 s. Probe trial performance is expressed as the percentage of time spent in each quadrant of the MWM.

2.5. Statistics

Baseline polysomnographic recordings and MWM acquisition data were analyzed using mixed design ANOVA. Genotype differences per age group were further assessed with Student's *t*-test. Similarly, mixed design ANOVA was used to analyze ambulatory cage activity. Then, phase differences were assessed with paired samples *t*-test and genotype differences with independent samples *t*-test. Spectral genotype-related differences in the EEG were assessed using independent samples *t*-test for every separate vigilance parameter. ANOVA with post-hoc Bonferroni correction was used to identify age differences in fronto-parietal ratio parameters, while independent samples *t*-tests served to identify differences between genotypes. All statistical results were considered significant for a value of $p < 0.05$, unless stated otherwise. Statistical calculations were performed using SPSS 24 (IBM, SPSS Inc., Chicago, IL, USA).

3. Results

3.1. Hippocampus-dependent learning was affected from 6 months of age

An overall mixed design ANOVA revealed an overall gradual decrease in path length ($F(7, 413) = 50.329$; $p = .000$) and latency ($F(7, 413) = 92.671$; $p = .000$) over all eight acquisition trials, demonstrating an appropriate learning curve for all animals. Also, the statistical model showed that for both path length and escape latency there was an effect of age (path length: $F(2, 59) = 3.222$; $p = .047$; escape latency: $F(2, 59) = 7.731$; $p = .001$), genotype (path length: $F(1, 59) = 18.212$; $p = .000$; escape latency: $F(1, 59) = 20.261$; $p = .000$) as well as an interaction effect between age and genotype (path length: $F(2, 59) = 3.497$; $p = .037$; escape latency: $F(2, 59) = 3.445$; $p = .038$). Velocity was affected by age ($F(2, 59) = 10.715$; $p = .000$) but not by genotype ($F(1, 59) = 0.609$; $p = .438$). To reduce the complexity of the data, genotype and trial effects were assessed by applying a mixed model per age group.

Genotype had no effect on path length ($F(1, 19) = 0.068$; $p = .797$) and escape latency ($F(1, 19) = 0.187$; $p = .670$) in 3-month-old animals. In addition, the profile of their learning curve was not significantly different between the different genotypes, since the interaction between trial and genotype was statistically non-significant ($p = .403$). Thus, young WT and HEM APP23 mice performed similarly in the MWM (Fig. 1).

At 6 months of age, APP23 mice swam a significantly longer distance (Fig. 1) and needed a significantly longer escape latency to reach the platform (Fig. 1) when compared to WT mice of the same age. Mixed design ANOVA revealed a significant effect of genotype on path length ($F(1, 20) = 13.852$; $p = .001$) and on escape latency ($F(1, 20) = 11.076$; $p = .003$). Moreover, the interaction of genotype with the different trials significantly influenced path length ($F(4.3, 86.9) = 3.271$; $p = .013$), but not escape latency ($F(4.075, 81.5) = 1.989$; $p = .103$). The genotype-related differences cannot be explained by a difference in swimming speed since the statistical model showed no effect of genotype on velocity ($F(1, 20) = 2.883$; $p = .105$).

Similarly, 12-month-old HEM mice needed more time to reach the platform and concurrently travelled a longer distance compared to WT littermates (Fig. 1). Genotype had a significant effect on path length ($F(1, 20) = 18.647$; $p = .000$) and escape latency ($F(1, 20) = 18.525$; $p = .000$). The interaction between genotype and trials was not significant for path length ($F(7, 140) = 2.023$; $p = .056$) and escape latency ($F(7; 140) = 1.874$; $p = .078$). Hence, the results show that old HEMs are definitely inferior in maze performance compared to old WTs, yet the profile of their learning curve is quite similar. Again, the results cannot be explained by differences in swim velocity ($F(1, 20) = .334$; $p = .570$).

Remarkably, no genotype-related differences could be demonstrated in the probe trial, even though the learning curves significantly differed between HEM and WT animals of 6 and 12 months of age. In spite of non-significance, 12-month-old HEM animals tend to spend less time in the target quadrant ($p = 0.075$), as can be visually observed in Fig. 1. An age-related effect for quadrant preference was observed. Here, 12-month-old mice spent significantly more time in the opposite quadrant compared to 6-month-old mice ($t = -2.723$; $p = .009$), indicating an altered searching pattern at old age.

Analyses of variance indicated that there were significant differences between the time spent in each quadrant ($p < 0.005$). Tukey post-hoc analyses always revealed significant differences between the time spent in the target quadrant and the opposite quadrant, except in 3-month-old and 12-month-old hemizygous mice. In all other groups, the time in the target quadrant always significantly differed from the time in the opposite quadrant and at least one other adjacent quadrant. Therefore, we believe that the animals definitely have an existent memory of the platform position. Remarkably, only 12-month-old hemizygous mice have no specific preference for any quadrant, given the lack of significant differences in time between all the different quadrants. This finding suggest that memory is severely affected in hemizygous mice of 12 months of age.

3.2. Cage activity hints towards hyperactivity during the dark phase

During the polysomnographic recordings, ambulatory cage activity was tracked using infrared sensors. To ensure decent habituation of the animals, only the third day of recording was included in the analysis (similar to the sleep analyses). We found that, at all ages, both genotypes exhibited a higher activity level in the dark period, the animal's active phase, than in the light phase ($t = -12.957$; $p = .000$).

We divided every 12 h light/dark block into smaller blocks of 6 h, resulting in 4 main time blocks: L1 (08:00-14:00), L2 (14:00-20:00), D1 (20:00-02:00) and D2 (02:00-08:00). The total light phase was indicated as 'L', the total dark phase as 'D'. An overall aging effect was present ($F(2, 36) = 5.315$; $p = 0.009$)., which was most noticeable in the light phase (L: $F(2, 47) = 5.725$; $p = .006$, L1: $F(2, 48) = 5.254$; $p = .009$, L2: $F(2, 48) = 5.491$; $p = .007$). The cage activity plots (Fig. 2) demonstrated that WT animals had a high cage activity level at three months, which gradually decreased with aging, while HEM mice had a similar activity profile at 3 and 6 months and became hyperactive in the dark phase at 12 months of age. Evidently, 12-month-old HEM APP23 mice were significantly more active than WT littermates during the D1 phase ($t = -3.534$; $p = .003$) and the whole dark phase ($t = -2.484$; $p = .029$). Additionally, a significant difference was observed in the D1 phase of 3-month-old mice ($t = -2.442$; $p = .028$), which is due to the fact that young WT mice are more active during the first part of the night than HEM mice. Independent samples *t*-test identified no significant genotype differences at 6 months of age. Hence, ambulatory cage activity is affected at an old age, at which HEM APP23 mice seem to be hyperaroused or hyperactive in the dark phase. Reversely, at a young age, WT mice appear to be more active than HEM mice.

3.3. Sleep architecture is affected at an older age but only during the dark phase

Polysomnographic data allowed us to quantify the total amount of time the mice spent awake or in NREM and REM sleep during the light and dark phase, as well as the average episode/bout duration. All mice displayed a preference for sleep during the light phase (NREM: $F(1, 59) = 429.880$; $p = .000$, REM: ($F(1, 59) = 863.019$; $p = .000$, wake: ($F(1, 59) = 1536.032$; $p = .000$). Also, average episode duration of all vigilance stages was significantly dependent on the light-dark cycle (NREM: $F(1, 59) = 203.673$; $p = .000$, REM: ($F(1, 59) = 11.286$; $p = .001$, wake: ($F(1, 59) = 90.157$; $p = .000$).

In both WT and HEM APP23 mice, the sleep-wake architecture undergoes changes with aging. Bout duration of all vigilance states significantly differs during the course of aging (NREM: F(2,

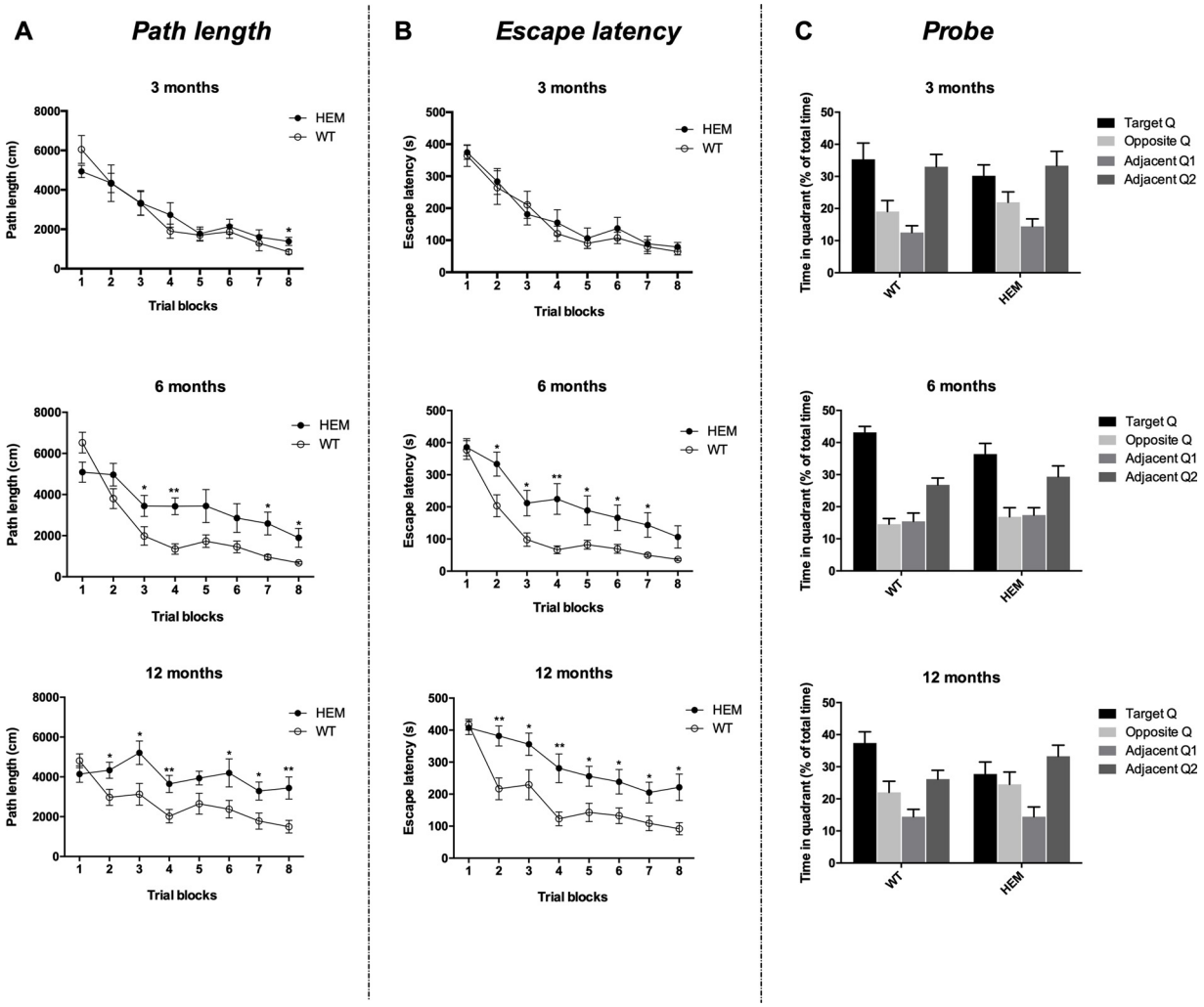

Fig. 1. Morris water maze performance of APP23 mice is affected at 6 months of age. Path length (A) and escape latency (B) of hemizygous (HEM) APP23 mice (closed symbols) and wild-type (WT) littermates (open symbols) during acquisition trial blocks in the hidden-platform MWM experiment at 3 (WT: $n = 10$, HEM: $n = 11$), 6 (WT: $n = 12$, HEM: $n = 10$) and 12 months (WT: $n = 11$, HEM: $n = 11$) of age. Also, the time spent in each quadrant during probe trial is shown (C). Asterisks indicate significant genotype difference as assessed by post-hoc independent samples Student's *t*-test; $*p < 0.05$, $**p < 0.01$.

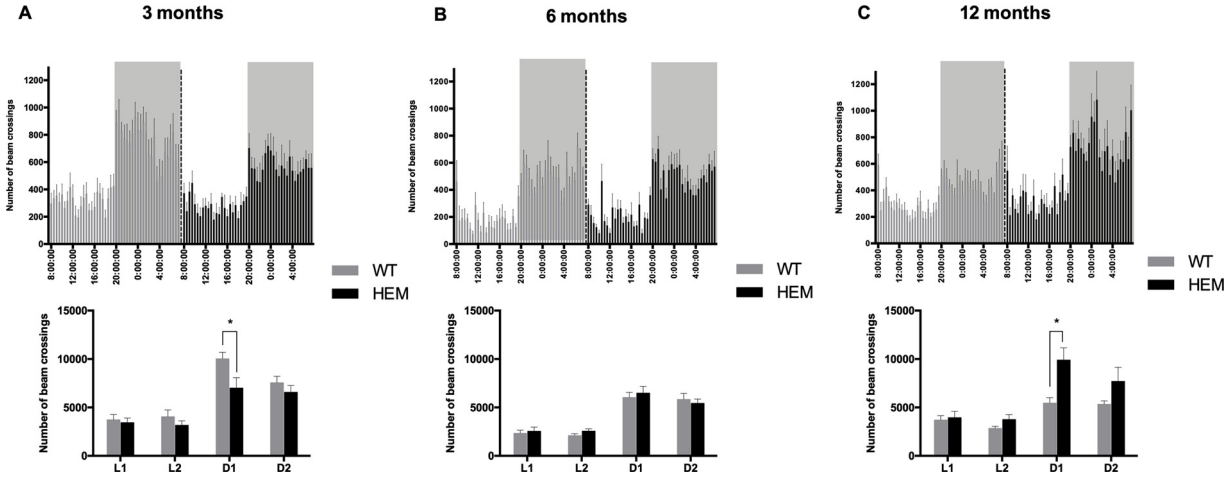

Fig. 2. Ambulatory cage activity demonstrates that HEM APP23 mice are hyperactive at old age. Cage activity profile of the last 24 h of the polysomnographic recording in (**A**) 3-month-old (WT: $n = 10$, HEM: $n = 9$), (**B**) 6-month-old (WT: $n = 11$, HEM: $n = 10$) and (**C**) 12-month-old (WT: $n = 11$, HEM: $n = 11$) mice. Bars represent mean (± SEM) summed number of beam crossings within a 30-minute interval. Shaded background represents the dark active phase of the animals' 12 h/12 h day/night cycle (lights on at 8 a.m.).

Table 1
Average wake episode duration is longer during the dark phase at 12 months of age in APP23 mice.

		3 M		6 M		12 M	
		WT (n = 10)	HEM (n = 11)	WT (n = 12)	HEM (n = 10)	WT (n = 11)	HEM (n = 11)
NREM BD	*Light*	153.4 ± 17.2	160.10 ± 10.9	252.1 ± 9.3	225.5 ± 12.1	159.9 ± 12.3	172.1 ± 16.3
	Dark	64.6 ± 3.8	54.7 ± 6.5	179.5 ± 6.4	172.3 ± 9.0	111.8 ± 8.3	95.0 ± 7.7
	Total	139.3 ± 14.6	147.5 ± 11.8	224.9 ± 7.3	208.7 ± 11.0	139.4 ± 10.3	143.8 ± 12.8
REM BD	*Light*	76.0 ± 5.5	71.2 ± 4.2	73.0 ± 2.6	80.09 ± 2.4	82.7 ± 3.6	83.8 ± 3.0
	Dark	60.6 ± 2.4	64.2 ± 4.6	66.5 ± 4.5	74.6 ± 5.8	74.3 ± 4.7	78.5 ± 7.3
	Total	71.9 ± 4.2	69.5 ± 3.8	71.7 ± 2.4	78.3 ± 2.2	80.0 ± 3.4	81.8 ± 2.6
Wake BD	*Light*	182.7 ± 26.1	211.9 ± 26.0	218.3 ± 15.9	196.2 ± 19.9	186.1 ± 18.3	198.1 ± 24.4
	Dark	669.8 ± 83.7	1049.9 ± 234.4	639.1 ± 80.9	818.3 ± 167.3	**351.0 ± 37.7***	511.6 ± 58.9
	Total	353.5 ± 49.1	438.6 ± 61.7	404.2 ± 35.6	408.2 ± 43.0	261.7 ± 24.0	328.0 ± 36.3

Bout duration (BD) during the dark-light phase for every included group. At 12 months of age (12 M), hemizygous (HEM) APP23 mice had longer waking episodes in the dark phase than wild-type (WT) littermates, thereby confirming a probable hyperactive state during this period. At other stages of pathology (3 M and 6 M) no significant differences were found. Data are presented as mean ± SEM. Genotype differences were assessed with an independent samples Student's *t*-test (* *p*-value < 0.05).

59) = 72.895; $p = .000$, REM: (F(2, 59) = 6.141; $p = .001$, wake: (F(2, 59) = 5.209; $p = .000$) (Table 1). Concurrently, age had an effect on the total wake time (F(2, 59) = 33.519; $p = .000$) and the total time spent in NREM (F(2, 59) = 35.968; $p = .000$). By contrast, REM sleep stays relatively well conserved F(2, 59) = 2.112; $p = .130$). Young 3-month-old mice were awake during about 63% of the day. At 6 months of age, wakefulness gradually decreased, but increased again at an older age of 12 months. Moreover, the difference in total wake duration between the light and dark phase (phase x age interaction) was most noticeable at the age of 6 months (F(2, 59) = 9.864; $p = .000$).

Mixed design ANOVA revealed genotype differences in total NREM time (F(1, 59) = 12.276; $p = .001$) and total wake time (F(1, 59) = 14.456; $p = .000$), and in wake bout duration (F(1, 59) = 4.723; $p = .034$). Also, the difference in time awake (F(1, 59) = 7.998; $p = .006$) and wake bout duration (F(1, 59) = 5.463; $p = .023$) between light and dark phase were more pronounced in HEM APP23 mice. Post-hoc independent samples *t*-test unveiled that 3-month-old HEM APP23 mice are slightly more awake than WT littermates, even though this difference was only borderline significant ($t = -2.119$; $p = .047$). More pronounced genotype differences were found at the older age of 12 months. At this stage of pathology, total NREM ($t = 2.713$; $p = .013$), REM ($t = 2.542$; $p = .019$), and wake ($t = -3.161$; $p = .005$) time were all significantly affected. Remarkably, these differences were a result of disturbed sleep patterns during the dark phase alone. NREM and REM sleep was decreased during the dark phase by respectively 35% and 55% (NREM: $t = 5.093$; $p = .000$, REM: $t = 5.405$; $p = .000$), while wakefulness was increased by 16% ($t = -5.896$; $p = .000$) (Fig. 3). Additionally, 12-month-old HEM mice displayed significant longer wake episodes during the dark phase ($t = -2.297$; $p = .033$) (Table 1). In the light phase, no genotype-related differences could be observed.

However, we observed that in the light phase (L), which was further subdivided into L1 (08:00–14:00) and L2 (14:00–20:00), sleep was significantly more fragmented in 6-month-old (L: $t = -3.692$; $p = .002$, L1: $t = -4.094$; $p = .001$, L2: $t = -2.224$; $p = .039$) and 12-month-old (L: $t = -2.622$; $p = .019$, L1: $t = -2.719$; $p = .015$, L2: $t = -2.180$; $p = .045$) HEM mice. Thus, sleep fragmentation already occurred at 6 months of age, and appeared much earlier than quantitative changes in sleep. Sleep fragmentation was also more pronounced in the L1 phase than in the L2 phase.

To investigate the relationship between sleep and cognition, Pearson correlation between MWM performance and sleep was calculated. Total sleep time (total NREM and REM time combined) significantly inversely correlated with learning disability, defined as the path length on trial 8 ($r = -0.417$, $n = 65$, $p = 0.001$).

3.4. Spectral power of brain oscillatory activity in APP23 mice is shifted towards higher frequencies

Quantitative EEG measures are increasingly considered as a potential biomarker for AD. In AD patients, a slowing of the EEG during wakefulness and REM has been demonstrated [31,32]. By contrast, not many transgenic models mimic these features. Therefore, we determined spectral EEG power for all three different vigilance states, in order to characterize the brain oscillatory activity of the APP23 model.

In this analysis, we focus on the parietal EEG, since frontal EEG might contain artifacts such as chewing and ocular contamination. At 3 months, almost no genotype differences in parietal EEG power were found. Differences in power spectra in wake and NREM only arose from 6 months of age. In wake, delta power was decreased ($t = 3.765$; $p =$

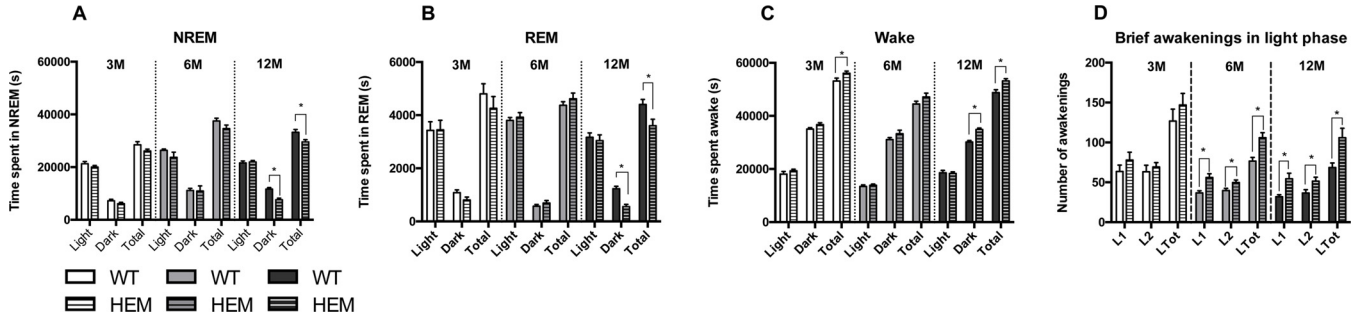

Fig. 3. Sleep architecture majorly deteriorates from 12 months of age in APP23 mice. The average time wild-type (WT) and hemizygous (HEM) APP23 mice spent in each vigilance state (**(A)** NREM, **(B)** REM and **(C)** wake) at different stages of pathology (3 M WT: $n = 10$, 3 M HEM: $n = 11$, 6 M WT: $n = 12$, 6 M HEM: $n = 10$, 12 M WT: $n = 11$, 12 M HEM: $n = 11$) throughout the light-dark phase. Bars represent mean (± SEM) time spent in the indicated vigilance state. Additionally, the number of brief awakenings during the light phase (LTot), divided into 2 period blocks of 6 h (L1 and L2), is displayed **(D)**.

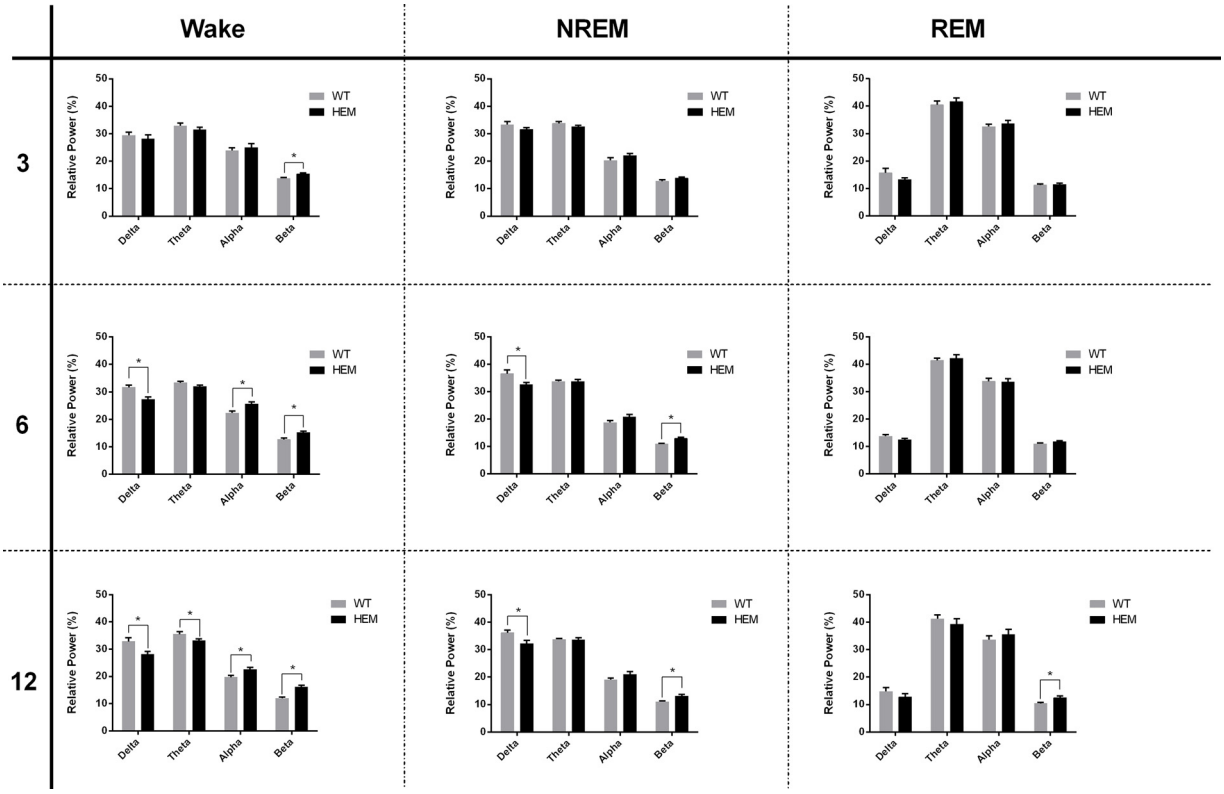

Fig. 4. Average wake episode duration is longer during the dark phase at 12 months of age in APP23 mice. Delta (0.5–3.5 Hz), theta (3.5–7.5 Hz), alpha (7.5–12.5 Hz) and beta (12.5–30 Hz) band power expressed relatively to the sum of all band power values (%). Data were depicted per age group (3 months: WT: $n = 9$, HEM: $n = 9$; 6 months: WT: $n = 8$, HEM: $n = 8$; 12 months: WT: $n = 9$, HEM: $n = 9$) and per vigilance state (NREM, REM and wake). Genotype differences were assessed by means of post-hoc independent samples Student's *t*-test. Bars represent mean (± SEM), * p-value < 0.05.

.002), while alpha ($t = -2.920$; $p = .011$) and beta power ($t = -3.190$; $p = .007$) were increased in HEM APP23 mice of 6 months. At 12 months, delta ($t = -2.659$; $p = .017$) and theta ($t = -2.241$; $p = .040$) power were decreased, while alpha (t = -2.980; $p = .009$) and beta ($t = -5.188$; $p = .000$) power were increased. Thus, in wake, parietal EEG power progressively shifts with age. In NREM sleep, delta power was decreased while beta power was increased in 6-month-old (delta: $t = 2.560$; $p = .023$; beta: $t = -3.832$; $p = .002$) and 12-month-old mice (delta: $t = 2.802$; $p = .013$; beta: $t = -2.765$; $p = .014$). In REM sleep, EEG power was relatively well conserved between genotypes across aging. Only at 12 months, beta power was significantly elevated in HEM mice ($t = -2.815$; $p = .012$) (Fig. 4).

Remarkably, only WT animals displayed a shift in oscillatory brain activity with age. Alpha and beta activity shifted during wake, with less alpha ($F(2,23) = 7.415$; $p = 0.003$) and beta ($F(2,23) = 5.299$; $p = 0.013$) power with increasing age. During NREM sleep, only beta activity decreased ($F(2,23) = 7.421$; $p = 0.003$). No age-related differences could be observed during REM sleep. By consequence, the genotype differences in spectral power at later ages are also partly caused by the shift towards slower oscillations in WT animals, that is absent in hemizygous animals (Fig. 4).

Furthermore, we observed a fronto-parietal gradient in delta power during NREM sleep that differed with age and genotype (Fig. 5). At a young age of 3 months, there was a frontal predominance of low frequency (0.5–4 Hz) delta power during NREM, since the fronto-parietal ratio was above 100%, confirming previous studies in rodents [33–36]. With aging, the frontal predominance disappeared ($F(2, 49) = 11.698$; $p = .000$). Moreover, a genotype effect was present, where HEM APP23 mice have a tendency towards a reduced frontal delta predominance during NREM. This difference was statistically significant at 6 months of age ($t = -2.236$; $p = .042$) and borderline significant at 12 months ($t = -1.884$; $p = .078$).

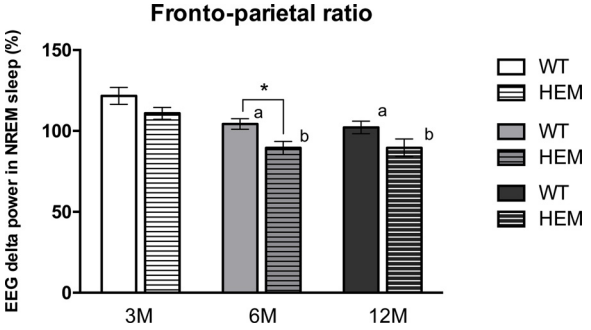

Fig. 5. Reduced frontal predominance with aging. The ratio of relative delta power in NREM sleep in the frontal cortex to that in parietal cortex, which demonstrates the regional dominance of delta power during NREM sleep. Power values above 100% indicate a frontal predominance, while power values below that indicate a parietal dominance. The letters 'a' and 'b' indicate age-related differences, where 'a' means significant different from 3-month-old (3 M) wild-type (WT) mice and 'b' fom 3 M hemizygous (HEM) mice, as assessed by post hoc independent samples Student's *t*-test with Bonferroni correction ($p < 0.0167$). Genotype differences were also analyzed with post-hoc independent samples Student's *t*-test (* p-value < 0.05). Bars represent mean (± SEM) delta power during NREM sleep (3 M: WT: $n = 9$, HEM: $n = 9$; 6 M: WT: $n = 8$, HEM: $n = 8$; 12 M: WT: $n = 9$, HEM: $n = 9$).

The frontal/parietal ratio of delta power during NREM sleep also significantly correlated with the difference in path length in trial 1 and trial 8 ($r = 0.460$, $n = 42$, $p = 0.001$). This suggests that frontal predominance of delta power during sleep might exert an effect on the learning abilities of these mice.

4. Discussion

4.1. Sleep and cognition

The APP23 amyloidosis mouse model displays severe sleep and activity disturbances during the dark, active phase, but only at an advanced stage of pathology. Although no individual pathological assessments have been included into analyses, the evolution of the pathology in this model has been thoroughly characterized [19–21]. At the onset of plaque deposition, at 6 months, already slight sleep architectural changes could be noted, such as a more fragmented pattern. However, no notable reduction in TST or time awake could be demonstrated at this stage. At 12 months of age, however, when amyloid plaques are diffusely present in the neocortex and hippocampus, NREM and REM sleep time were significantly reduced, while wakefulness was significantly increased. These alterations were a result of disturbances during the dark phase alone, suggesting a hyperaroused state during the active phase. Cage activity recordings, wherein 12-month-old animals also displayed hyperactivity during the dark phase, confirmed these findings. The course of sleep architectural changes is grossly parallel to the course of cognitive decline. Sleep fragmentation is apparent from 6 months onwards, when also MWM performance is severely affected. When pathology advances, and cognition even further deteriorates, also sleep function becomes progressively worse. Additionally, a correlation was established between total TST and the ability to learn. This correlation might be a direct result of amyloid pathology itself, where amyloid causes a deterioration of both sleep and cognition. However, it might also be a sign of a positive feedback loop at work, in which reduced sleep again has a negative effect on cognitive performance, since sleep processes are presumed to participate in memory consolidation, an active process that relies on reactivation and reorganization of newly encoded representations [17]. Of note, sleep disturbances are a hallmark symptom of depression, and sleep issues also increase one's risk for depression [37]. Like sleep disturbances, depressive symptoms arise early in the course of the disease [38], and both symptoms have also been identified as possible risk factors for AD [39]. Possibly, initial Aβ toxicity might disrupt pathways that are involved in both depression and sleep, causing these symptoms to coincide in the prodromal stage [40].

With aging, the TST reduces in the APP23 model. Generally, 12-month-old mice sleep less than 6-month-old mice. By contrast, 3-month-old mice sleep the least, although this could be a sign of the reduced sleep time often observed during adolescence [41]. Correspondingly, an age-related decline of TST has been demonstrated in human subjects [42–44].

The sleep architecture of AD patients is more deteriorated than that of age-matched control individuals. Already at early stages of the disease, AD patients (with a mean MMSE score around 23) have SWS reductions and experience longer and more frequent nocturnal awakenings [45]. With advancing severity of the disease, sleep fragmentation and SWS reduction aggravate and co-occur with REM sleep reductions [3,6,7,46]. Study finds that waking and REM measures are the strongest predictors of cognitive performance. Night-time wakefulness and REM sleep consistently predicted significant variance in cognitive and functional status measures in a large sample of community-dwelling AD patients [47]. APP23 mice of 6 months old exhibited a more fragmented sleep pattern during the light phase, although reductions in sleep or wake time could not be demonstrated yet. At this stage, cognitive performance was already affected. At a more advanced stage (12 months), sleep fragmentation coincided with NREM and REM reductions, along with further cognitive impairment. Hence, the onset of sleep disturbances in the APP23 model emerges quite early in the disease process. Sleep disturbances start moderately (namely with increased fragmentation) but progressively worsen, ultimately with reductions of SWS and REM sleep. Additionally, these sleep-wake alterations parallel cognitive decline. In conclusion, the APP23 model mimics the clinical situation well concerning the onset and progression of sleep disturbances and their relation with cognitive disabilities.

Remarkably, increased wakefulness and reduced sleep time (at advanced stages of pathology) are only present during the dark (i.e. active) phase, and not during the light phase. Together with the fact that ambulatory cage activity is higher in the dark [48], these findings suggest that old APP23 mice are hyperactive in their active period. This might correspond to the sundowning phenomenon in AD patients, in which symptoms (agitation, activity) are aggravated around dawn. Since the sleep-wake cycle is organized in a 'flip-flop' system [49] and mice exhibit a polyphasic sleep pattern, we are unable to determine whether this disruption is caused by the dysfunction of either wake- or sleep-promoting circuits. Either adrenergic or serotonergic branches of the reticular activating system might be overactive, or the galaninergic ventrolateral preoptic nucleus fails to inhibit this wake-promoting system. Lesions of the VLPO in rodents result in marked sleep fragmentation and a decrease of total sleep time, similar to the observed phenotype in the APP23 model [50]. Additionally, a study in the Tg2576 amyloidosis model has indicated that a cholinergic deficit has functional consequences for the EEG and for sleep regulation. Possibly, functional loss of the VLPO and nucleus basalis contributes to sleep loss and sleep fragmentation in both the APP23 model and AD patients [51]. Because of the polyphasic sleep pattern of mice and the uniphasic sleep of humans, it is quite difficult to encompass the light-dark differences within the clinical situation. Moreover, other AD mouse models do not uniformly display an increased wakefulness during the dark phase. Some reports indicate an increased wakefulness that is more pronounced during the dark phase [52,53], others during the light phase [16]. NREM and REM sleep was even conserved in the Tg2576 model up to 17 months [54]. These data demonstrate the dissension between the different models, of which the underlying cause remains currently unknown.

4.2. Spectral EEG components and their relation with sleep function

In AD patients, an overall slowing of the EEG has been demonstrated [31,32]. Moreover, this phenomenon has been increasingly considered as a potential biomarker for AD. However, many transgenic AD mouse models fail to recapitulate this EEG characteristic, since EEG slowing is probably caused by a loss of functional connectivity between cortical regions as a result of neurodegeneration and cholinergic deficits [32], while these manifestations are rather limited in transgenic mice [55]. Instead, most studies in amyloidosis models report an EEG power shift towards fast-frequency oscillations [52–54].

In the APP23 model, a similar tendency towards fast frequencies was found. Furthermore, this spectral shift appeared to progress with age. This progressive nature was best observed during wakefulness. At 3 months, genotype-related differences were relatively minor and only beta power was significantly increased in HEM APP23 mice. At 6 months, delta power was decreased, while alpha and beta power were increased. In 12-month-old HEM APP23 mice, all power bands were significantly different from WT littermates, including the theta band. This tendency towards fast frequencies is potentially a characteristic specific to mouse models that present with an overload of amyloid in the absence of neurodegeneration. What factors lie at the basis of this network desynchronization is currently unknown. In vitro experiments have demonstrated that Aβ can cause desynchronization of action potential generation in pyramidal cells and a general shift of the balance between excitation and inhibition in the hippocampal circuitry [56]. Recently, Aβ has been demonstrated to morphologically distort neurites in the barrel cortex of APP/PS1 mice, which is hypothesized to disrupt the precise temporal firing patterns in the neural network [57]. Similar findings were reported in post-mortem AD brains, where a neuron receiving input from dendrites that traverse an Aβ deposit would take longer to reach threshold for an action potential compared to input from dendrites that did not traverse an Aβ deposit [58]. The induced

curvature probably reduces the synchrony of converging inputs (jitter), leading to increased response variability of the neuron [59]. The resultant breakdown in synchronicity of timing could disrupt the functional integration of memory retrieval [58]. With respect to aforementioned data, additional clinical studies could be rewarding. In contrast, PLB1-triple mice, which represent an early-stage phenotype, display an age-dependent shift towards lower frequencies, as opposed to our findings [60]. This model demonstrates that the presence of subtle amyloid and tau pathology is sufficient to cause changes in sleep architecture and EEG spectra. However, the impact of the triple mutation and the tau pathology may not be underestimated, and therefore it proves difficult to translate these findings to the APP23 model.

A more desynchronous state during wakefulness in HEM APP23 mice might also indicate that these mice are more exploring when awake, while the WT littermates are more quiescent. It has been demonstrated that APP23 mice are more agitated and exploratory from a young age [61,62]. However, differences in cage activity patterns could only be demonstrated at the age of 12 months, while spectral differences were already obvious at 6 months. The observed decrease of delta power during wakefulness from 6 months of age might also be reflected on the sleep-wake function of the animal. Waking delta power is often considered to be a marker of sleep pressure [63]. Therefore, sleep fragmentation, and reduced sleep time at an older age, might be a result of the mice being less 'sleepy'. Moreover, NREM delta power, a proposed marker for sleep intensity, was also significantly lower. Less intense and less deep sleep results in faster awakenings. Hence, a more fragmented sleep pattern in HEM APP23 mice is possibly attributed to a reduced sleep propensity (and intensity), as suggested by a reduced delta power during wakefulness and NREM sleep. Recent studies in the APPswe/PSEN1dE9 model confirm these findings, and demonstrate an overall reduction of delta and theta power during NREM sleep [64,65]. Kent et al. reported no significant changes in total sleep time in this APP/PS1 model at the age of 12 months [64]. However, in depth analyses with separation of the light-dark photoperiod, revealed that these mice were more awake during the dark period and more asleep during the light period from 6 months, according to Zhang and others [65]. Therefore, the reduced delta power may also predict a disrupted sleep quality in this mouse model.

Remarkably, REM sleep power spectra stay relatively well conserved in the APP23 model. Although REM time is reduced by 55% at old age, the underlying neuronal firing appears grossly similar. Only beta power increased significantly. In accordance, Kent et al. could not demonstrate differences in the EEG spectra of REM sleep, while an obvious shift towards faster oscillations was present in both wake and NREM sleep in the APP/PS1 model [64]. By contrast, Zhang et al. showed a reduction of delta in theta power in REM spectra, similar to that observed during NREM sleep [65].

Since we observed spectral differences between frontal and parietal EEG leads, we scrutinized these differences by analyzing the power ratio between these two regions. In-depth analyses revealed that, at a young age, there is a frontal predominance of relative delta power, which disappeared with age. Most notably, HEM mice had a tendency towards a reduced fronto-parietal ratio. In human subjects, the fronto-occipital gradient decreases with age [66]. Additionally, in healthy aged volunteers, delta power is dominant in the parietal regions [66]. According to human imaging studies, delta activity covaried negatively with regional cerebral blood flow (rCBF) and a decrease of rCBF in frontal regions might be associated with cortical arousal attenuation during sleep [67]. Thus, the diminished frontal predominance of delta activity can possibly be interpreted as an 'alleviated dampening' of cortical arousal during sleep, accounting for the increased sleep fragmentation observed in the model [68].

In healthy, elderly humans significant associations were found between NREM frontal delta power and task performance. Delta power in sleep was found to be positively linked to waking cerebral metabolic rate [69]. The significant correlation between an age-dependent decline of the NREM delta frontal/parietal gradient with the difference in path length in trial 1 and trial 8 suggests that frontal predominance of delta power during sleep might exert an effect on awake learning abilities.

To conclude, sleep disturbances in the APP23 mouse model manifest at the onset of cognitive deterioration. Initially, these sleep disturbances are mild. Sleep is more fragmented but abnormalities in TST have not emerged yet. When cognitive abilities deteriorate even further, sleep disturbances also progressively worsen, as was demonstrated by the loss of NREM and REM sleep at the age of 12 months. Cage activity recordings indicate that the quantitative reductions of sleep are probably due to a hyperaroused or agitated state during the dark phase at this age. However, along with more subtle sleep architectural changes such as sleep fragmentation, spectral parameters of the EEG, which can provide information about sleep quality, are changed long before these quantitative sleep reductions arise. Hence, before sleep time is quantitatively reduced, the quality of sleep is probably already affected. All together, the APP23 mouse model mimics the clinical situation well, and will therefore be valid for use in the development of sleep therapeutics for people with AD.

Acknowledgements

This work was financed by the Research Foundation Flanders, the Belgian Foundation for Alzheimer Research (SAO –FRA; grant #15002), Rotary International's 'Hope in Head', the agreement between Institute Born-Bunge and the University of Antwerp, the Medical Research Foundation Antwerp, the Thomas Riellaerts research fund, and Neurosearch Antwerp. The authors have no conflict of interest to declare.

References

[1] M. Moran, C.A. Lynch, C. Walsh, R. Coen, D. Coakley, B.A. Lawlor, Sleep disturbance in mild to moderate Alzheimer's disease, Sleep Med. 6 (4) (2005) 347–352.
[2] S. Beaulieu-Bonneau, C. Hudon, Sleep disturbances in older adults with mild cognitive impairment, Int. Psychogeriatr. IPA 21 (4) (2009) 654–666.
[3] D.L. Bliwise, M. Hughes, P.M. McMahon, N. Kutner, Observed sleep/wakefulness and severity of dementia in an Alzheimer's disease special care unit, J. Gerontol. Ser. A Biol. Sci. Med. Sci. 50 (6) (1995) M303–6.
[4] Y.L. Huang, R.Y. Liu, Q.S. Wang, E.J. Van Someren, H. Xu, J.N. Zhou, Age-associated difference in circadian sleep-wake and rest-activity rhythms, Physiol. Behav. 76 (4–5) (2002) 597–603.
[5] S.M. McCurry, R.G. Logsdon, L. Teri, L.E. Gibbons, W.A. Kukull, J.D. Bowen, W.C. McCormick, E.B. Larson, Characteristics of sleep disturbance in community-dwelling Alzheimer's disease patients, J. Geriatr. Psychiatry Neurol. 12 (2) (1999) 53–59.
[6] P.N. Prinz, E.R. Peskind, P.P. Vitaliano, M.A. Raskind, C. Eisdorfer, N. Zemcuznikov, C.J. Gerber, Changes in the sleep and waking EEGs of non-demented and demented elderly subjects, J. Am. Geriatr. Soc. 30 (2) (1982) 86–93.
[7] W. Witting, I.H. Kwa, P. Eikelenboom, M. Mirmiran, D.F. Swaab, Alterations in the circadian rest-activity rhythm in aging and Alzheimer's disease, Biol. Psychiatry 27 (6) (1990) 563–572.
[8] K.E. Moe, M.V. Vitiello, L.H. Larsen, P.N. Prinz, Symposium: cognitive processes and sleep disturbances: sleep/wake patterns in Alzheimer's disease: relationships with cognition and function, J. Sleep Res. 4 (1) (1995) 15–20.
[9] C.P. Pollak, D. Perlick, Sleep problems and institutionalization of the elderly, J. Geriatr. Psychiatry Neurol. 4 (4) (1991) 204–210.
[10] C.F. Hatfield, J. Herbert, E.J. van Someren, J.R. Hodges, M.H. Hastings, Disrupted daily activity/rest cycles in relation to daily cortisol rhythms of home-dwelling patients with early Alzheimer's dementia, Brain 127 (Pt 5) (2004) 1061–1074.
[11] Y.E. Ju, J.S. McLeland, C.D. Toedebusch, C. Xiong, A.M. Fagan, S.P. Duntley, J.C. Morris, D.M. Holtzman, Sleep quality and preclinical Alzheimer disease, JAMA Neurol. 70 (5) (2013) 587–593.
[12] S.M. McCurry, C.F. Reynolds, S. Ancoli-Israel, L. Teri, M.V. Vitiello, Treatment of sleep disturbance in Alzheimer's disease, Sleep Med. Rev. 4 (6) (2000) 603–628.
[13] T.W. Meeks, S.A. Ropacki, D.V. Jeste, The neurobiology of neuropsychiatric syndromes in dementia, Curr. Opin. Psychiatry 19 (6) (2006) 581–586.
[14] L. Xie, H. Kang, Q. Xu, M.J. Chen, Y. Liao, M. Thiyagarajan, J. O'Donnell, D.J. Christensen, C. Nicholson, J.J. Iliff, T. Takano, R. Deane, M. Nedergaard, Sleep drives metabolite clearance from the adult brain, Science (New York, N.Y.) 342 (6156) (2013) 373–377.
[15] J.E. Kang, M.M. Lim, R.J. Bateman, J.J. Lee, L.P. Smyth, J.R. Cirrito, N. Fujiki, S. Nishino, D.M. Holtzman, Amyloid-beta dynamics are regulated by orexin and the sleep-wake cycle, Science (New York, N.Y.) 326 (5955) (2009) 1005–1007.
[16] J.H. Roh, Y. Huang, A.W. Bero, T. Kasten, F.R. Stewart, R.J. Bateman,

D.M. Holtzman, Disruption of the sleep-wake cycle and diurnal fluctuation of beta-amyloid in mice with Alzheimer's disease pathology, Sci. Transl. Med. 4 (150) (2012) 150ra122.
[17] J. Born, B. Rasch, S. Gais, Sleep to remember, Neuroscientist 12 (5) (2006) 410–424.
[18] R.D. Nebes, D.J. Buysse, E.M. Halligan, P.R. Houck, T.H. Monk, Self-reported sleep quality predicts poor cognitive performance in healthy older adults, J. Gerontol. Ser. A Biol. Sci. Med. Sci. 64 (2) (2009) 180–187.
[19] D. Van Dam, E. Vloeberghs, D. Abramowski, M. Staufenbiel, P.P. De Deyn, APP23 mice as a model of Alzheimer's disease: an example of a transgenic approach to modeling a CNS disorder, CNS Spectr. 10 (3) (2005) 207–222.
[20] M.E. Calhoun, K.H. Wiederhold, D. Abramowski, A.L. Phinney, A. Probst, C. Sturchler-Pierrat, M. Staufenbiel, B. Sommer, M. Jucker, Neuron loss in APP transgenic mice, Nature 395 (6704) (1998) 755–756.
[21] C. Sturchler-Pierrat, D. Abramowski, M. Duke, K.H. Wiederhold, C. Mistl, S. Rothacher, B. Ledermann, K. Burki, P. Frey, P.A. Paganetti, C. Waridel, M.E. Calhoun, M. Jucker, A. Probst, M. Staufenbiel, B. Sommer, Two amyloid precursor protein transgenic mouse models with Alzheimer disease-like pathology, Proc. Natl. Acad. Sci. U. S. A. 94 (24) (1997) 13287–13292.
[22] J. Janssens, R.A.J. Crans, K. Van Craenenbroeck, J. Vandesompele, C.P. Stove, D. Van Dam, P.P. De Deyn, Evaluating the applicability of mouse SINEs as an alternative normalization approach for RT-qPCR in brain tissue of the APP23 model for Alzheimer's disease, J. Neurosci. Methods 320 (2019) 128–137.
[23] K.B.J. Franklin, G. Paxinos, The Mouse Brain in Stereotactic Coordinates, (2008).
[24] I. Tobler, T. Deboer, M. Fischer, Sleep and sleep regulation in normal and prion protein-deficient mice, J. Neurosci. 17 (5) (1997) 1869.
[25] T. Deboer, P. Franken, I. Tobler, Sleep and cortical temperature in the Djungarian hamster under baseline conditions and after sleep deprivation, J. Comp. Physiol. A Sens. Neural Behav. Physiol. 174 (2) (1994) 145–155.
[26] I. Tobler, S.E. Gaus, T. Deboer, P. Achermann, M. Fischer, T. Rulicke, M. Moser, B. Oesch, P.A. McBride, J.C. Manson, Altered circadian activity rhythms and sleep in mice devoid of prion protein, Nature 380 (6575) (1996) 639–642.
[27] C. Besthorn, H. Förstl, C. Geiger-Kabisch, H. Sattel, T. Gasser, U. Schreiter-Gasser, EEG coherence in Alzheimer disease, Electroencephalogr. Clin. Neurophysiol. 90 (3) (1994) 242–245.
[28] C.L. Ehlers, J.R. Criado, Event-related oscillations in mice: effects of stimulus characteristics, J. Neurosci. Methods 181 (1) (2009) 52–57.
[29] A.B.L. Tort, S. Ponsel, J. Jessberger, Y. Yanovsky, J. Brankačk, A. Draguhn, Parallel detection of theta and respiration-coupled oscillations throughout the mouse brain, Sci. Rep. 8 (1) (2018) 6432–6432.
[30] D. Van Dam, R. D'Hooge, M. Staufenbiel, C. Van Ginneken, F. Van Meir, P.P. De Deyn, Age-dependent cognitive decline in the APP23 model precedes amyloid deposition, Eur. J. Neurosci. 17 (2) (2003) 388–396.
[31] J. Goossens, J. Laton, J. Van Schependom, J. Gielen, H. Struyfs, S. Van Mossevelde, T. Van den Bossche, J. Goeman, P.P. De Deyn, A. Sieben, J.J. Martin, C. Van Broeckhoven, J. van der Zee, S. Engelborghs, G. Nagels, EEG dominant frequency peak differentiates between Alzheimer's disease and frontotemporal lobar degeneration, J. Alzheimer's Dis. JAD 55 (1) (2017) 53–58.
[32] J. Jeong, EEG dynamics in patients with Alzheimer's disease, Clin. Neurophysiol. 115 (7) (2004) 1490–1505.
[33] S. Palchykova, T. Deboer, I. Tobler, Selective sleep deprivation after daily torpor in the Djungarian hamster, J. Sleep Res. 11 (4) (2002) 313–319.
[34] B. Schwierin, P. Achermann, T. Deboer, A. Oleksenko, A.A. Borbély, I. Tobler, Regional differences in the dynamics of the cortical EEG in the rat after sleep deprivation, Clin. Neurophysiol. 110 (5) (1999) 869–875.
[35] V.V. Vyazovskiy, T. Deboer, B. Rudy, D. Lau, A.A. Borbely, I. Tobler, Sleep EEG in mice that are deficient in the potassium channel subunit K.v.3.2, Brain Res. 947 (2) (2002) 204–211.
[36] V.V. Vyazovskiy, G. Ruijgrok, T. Deboer, I. Tobler, Running wheel accessibility affects the regional electroencephalogram during sleep in mice, Cereb. Cortex (New York, N.Y.: 1991) 16 (3) (2006) 328–336.
[37] A. Kumar, P. Chanana, Sleep reduction: a link to other neurobiological diseases, Sleep Biol. Rhythms 12 (3) (2014) 150–161.
[38] B.C. Jost, G.T. Grossberg, The evolution of psychiatric symptoms in Alzheimer's disease: a natural history study, J. Am. Geriatr. Soc. 44 (9) (1996) 1078–1081.
[39] R.L. Ownby, E. Crocco, A. Acevedo, V. John, D. Loewenstein, Depression and risk for Alzheimer disease: systematic review, meta-analysis, and metaregression analysis, JAMA Psychiatry 63 (5) (2006) 530–538.
[40] F.S. Giorgi, L. Ryskalin, R. Ruffoli, F. Biagioni, F. Limanaqi, M. Ferrucci, C.L. Busceti, U. Bonuccelli, F. Fornai, The neuroanatomy of the reticular nucleus locus coeruleus in Alzheimer's disease, Front. Neuroanat. 11 (2017) 80–80.
[41] M.A. Carskadon, Sleep in adolescents: the perfect storm, Pediatr. Clin. North Am. 58 (3) (2011) 637–647.
[42] I. Feinberg, V.R. Carlson, Sleep variables as a function of age in man, Arch. Gen. Psychiatry 18 (2) (1968) 239–250.
[43] B.A. Mander, J.R. Winer, M.P. Walker, Sleep and human aging, Neuron 94 (1) (2017) 19–36.
[44] S. Redline, H.L. Kirchner, S.F. Quan, D.J. Gottlieb, V. Kapur, A. Newman, The effects of age, sex, ethnicity, and sleep-disordered breathing on sleep architecture, Arch. Intern. Med. 164 (4) (2004) 406–418.
[45] M.V. Vitiello, P.N. Prinz, Alzheimer's disease. Sleep and sleep/wake patterns, Clin. Geriatr. Med. 5 (2) (1989) 289–299.
[46] M.V. Vitiello, J.A. Bokan, W.A. Kukull, R.L. Muniz, R.G. Smallwood, P.N. Prinz, Rapid eye movement sleep measures of Alzheimer's-type dementia patients and optimally healthy aged individuals, Biol. Psychiatry 19 (5) (1984) 721–734.
[47] K.E. Moe, M.V. Vitiello, L.H. Larsen, P.N. Prinz, Sleep/wake patterns in Alzheimer's disease: relationships with cognition and function, J. Sleep Res. 4 (1) (1995) 15–20.
[48] E. Vloeberghs, D. Van Dam, S. Engelborghs, G. Nagels, M. Staufenbiel, P.P. De Deyn, Altered circadian locomotor activity in APP23 mice: a model for BPSD disturbances, Eur. J. Neurosci. 20 (10) (2004) 2757–2766.
[49] C.B. Saper, T.E. Scammell, J. Lu, Hypothalamic regulation of sleep and circadian rhythms, Nature 437 (7063) (2005) 1257–1263.
[50] J. Lu, M.A. Greco, P. Shiromani, C.B. Saper, Effect of lesions of the ventrolateral preoptic nucleus on NREM and REM sleep, J. Neurosci. 20 (10) (2000) 3830–3842.
[51] A.S. Lim, B.A. Ellison, J.L. Wang, L. Yu, J.A. Schneider, A.S. Buchman, D.A. Bennett, C.B. Saper, Sleep is related to neuron numbers in the ventrolateral preoptic/intermediate nucleus in older adults with and without Alzheimer's disease, Brain 137 (Pt 10) (2014) 2847–2861.
[52] J. Colby-Milley, C. Cavanagh, S. Jego, J.C. Breitner, R. Quirion, A. Adamantidis, Sleep-wake cycle dysfunction in the TgCRND8 mouse model of Alzheimer's disease: from early to advanced pathological stages, PLoS One 10 (6) (2015) e0130177.
[53] A. Jyoti, A. Plano, G. Riedel, B. Platt, EEG, activity, and sleep architecture in a transgenic AbetaPPswe/PSEN1A246E Alzheimer's disease mouse, J. Alzheimers Dis. 22 (3) (2010) 873–887.
[54] J.P. Wisor, D.M. Edgar, J. Yesavage, H.S. Ryan, C.M. McCormick, N. Lapustea, G.M. Murphy Jr., Sleep and circadian abnormalities in a transgenic mouse model of Alzheimer's disease: a role for cholinergic transmission, Neuroscience 131 (2) (2005) 375–385.
[55] O. Wirths, T.A. Bayer, Neuron loss in transgenic mouse models of Alzheimer's disease, Int. J. Alzheimers Dis. 2010 (2010).
[56] F.R. Kurudenkandy, M. Zilberter, H. Biverstal, J. Presto, D. Honcharenko, R. Stromberg, J. Johansson, B. Winblad, A. Fisahn, Amyloid-beta-induced action potential desynchronization and degradation of hippocampal gamma oscillations is prevented by interference with peptide conformation change and aggregation, J. Neurosci. 34 (34) (2014) 11416–11425.
[57] S. Beker, M. Goldin, N. Menkes-Caspi, V. Kellner, G. Chechik, E.A. Stern, Amyloid-β disrupts ongoing spontaneous activity in sensory cortex, Brain Struct. Funct. 221 (2) (2016) 1173–1188.
[58] R.B. Knowles, C. Wyart, S.V. Buldyrev, L. Cruz, B. Urbanc, M.E. Hasselmo, H.E. Stanley, B.T. Hyman, Plaque-induced neurite abnormalities: implications for disruption of neural networks in Alzheimer's disease, Proc. Natl. Acad. Sci. U. S. A. 96 (9) (1999) 5274–5279.
[59] E.A. Stern, B.J. Bacskai, G.A. Hickey, F.J. Attenello, J.A. Lombardo, B.T. Hyman, Cortical synaptic integration in vivo is disrupted by amyloid-β plaques, J. Neurosci. 24 (19) (2004) 4535.
[60] A. Jyoti, A. Plano, G. Riedel, B. Platt, Progressive age-related changes in sleep and EEG profiles in the PLB1Triple mouse model of Alzheimer's disease, Neurobiol. Aging 36 (10) (2015) 2768–2784.
[61] A. Pfeffer, T. Munder, S. Schreyer, C. Klein, J. Rasinska, Y. Winter, B. Steiner, Behavioral and psychological symptoms of dementia (BPSD) and impaired cognition reflect unsuccessful neuronal compensation in the pre-plaque stage and serve as early markers for Alzheimer's disease in the APP23 mouse model, Behav. Brain Res. 347 (2018) 300–313.
[62] Y. Senechal, L. Prut, P.H. Kelly, M. Staufenbiel, F. Natt, D. Hoyer, C. Wiessner, K.K. Dev, Increased exploratory activity of APP23 mice in a novel environment is reversed by siRNA, Brain Res. 1243 (2008) 124–133.
[63] R. Huber, T. Deboer, I. Tobler, Effects of sleep deprivation on sleep and sleep EEG in three mouse strains: empirical data and simulations, Brain Res. 857 (1–2) (2000) 8–19.
[64] B.A. Kent, M. Michalik, E.G. Marchant, K.W. Yau, H.H. Feldman, R.E. Mistlberger, H.B. Nygaard, Delayed daily activity and reduced NREM slow-wave power in the APPswe/PS1dE9 mouse model of Alzheimer's disease, Neurobiol. Aging 78 (2019) 74–86.
[65] F. Zhang, R. Zhong, S. Li, Z. Fu, R. Wang, T. Wang, Z. Huang, W. Le, Alteration in sleep architecture and electroencephalogram as an early sign of Alzheimer's disease preceding the disease pathology and cognitive decline, Alzheimer's Dement. 15 (4) (2019) 590–597.
[66] H.P. Landolt, A.A. Borbely, Age-dependent changes in sleep EEG topography, Clin. Neurophysiol. 112 (2) (2001) 369–377.
[67] N. Hofle, T. Paus, D. Reutens, P. Fiset, J. Gotman, A.C. Evans, B.E. Jones, Regional cerebral blood flow changes as a function of delta and spindle activity during slow wave sleep in humans, J. Neurosci. 17 (12) (1997) 4800.
[68] M. Munch, V. Knoblauch, K. Blatter, C. Schroder, C. Schnitzler, K. Krauchi, A. Wirz-Justice, C. Cajochen, The frontal predominance in human EEG delta activity after sleep loss decreases with age, Eur. J. Neurosci. 20 (5) (2004) 1402–1410.
[69] C. Anderson, J.A. Horne, Prefrontal cortex: links between low frequency delta EEG in sleep and neuropsychological performance in healthy, older people, Psychophysiology 40 (3) (2003) 349–357.